

All our information about the physical properties of stars comes more or less directly from studies of their spectra. In particular, by studying the strength of various absorption lines, stellar masses, temperatures and compositions can be deduced. The line shapes contain detailed information about atmospheric processes.

As we have seen in Chap. 3, the light of a star can be dispersed into a spectrum by means of a prism or a diffraction grating. The distribution of the energy flux density over frequency can then be derived. The spectra of stars consist of a *continuous spectrum* or *continuum* with narrow *spectral lines* superimposed (Fig. 9.1). The lines in stellar spectra are mostly dark *absorption lines*, but in some objects bright *emission lines* also occur.

In a very simplified way the continuous spectrum can be thought of as coming from the hot surface of the star. Atoms in the atmosphere above the surface absorb certain characteristic wavelengths of this radiation, leaving dark “gaps” at the corresponding points in the spectrum. In reality there is no such sharp separation between surface and atmosphere. All layers emit and absorb radiation, but the net result of these processes is that less energy is radiated at the wavelengths of the absorption lines.

The spectra of stars are classified on the basis of the strengths of the spectral lines. *Isaac Newton* observed the solar spectrum in 1666, but, properly speaking, spectroscopy began in 1814 when *Joseph Fraunhofer* observed the dark lines in the spectrum of the Sun. He assigned capi-

tal letters, like D, G, H and K, to some of the stronger dark lines without knowing the elements responsible for the origin of the lines (Sect. 9.2). The absorption lines are also known as *Fraunhofer lines*. In 1860, *Gustav Robert Kirchhoff* and *Robert Bunsen* identified the lines as the characteristic lines produced by various elements in an incandescent gas.

---

## 9.1 Measuring Spectra

The most important methods of forming a spectrum are by means of an objective prism or a slit spectrograph. In the former case one obtains a photograph, where each stellar image has been spread into a spectrum. Up to several hundred spectra can be photographed on a single plate and used for spectral classification. The amount of detail that can be seen in a spectrum depends on its *dispersion*, the range of wavelengths per millimetre on the plate (or per pixel on a CCD). The dispersion of an objective prism is a few tens of nanometres per millimetre. More detailed observations require a slit spectrograph, which can reach a dispersion 1–0.01 nm/mm. The detailed shape of individual spectral lines can then be studied.

The photograph of the spectrum is converted to an intensity tracing showing the flux density as a function of wavelength. This is done by means of a microdensitometer, measuring the amount of light transmitted by the recorded spectrum. Since the blackening of a photographic plate is not linearly related to the amount of energy it has re-

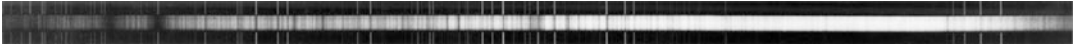


**Fig. 9.1** A typical stellar spectrum. The continuous spectrum is brightest at about 550 nm and gets fainter towards shorter and longer wavelengths. Dark absorption lines are

superimposed on the continuum. The spectrum of the star,  $\eta$  Pegasi, is very similar to that of our Sun. (Mt. Wilson Observatory)

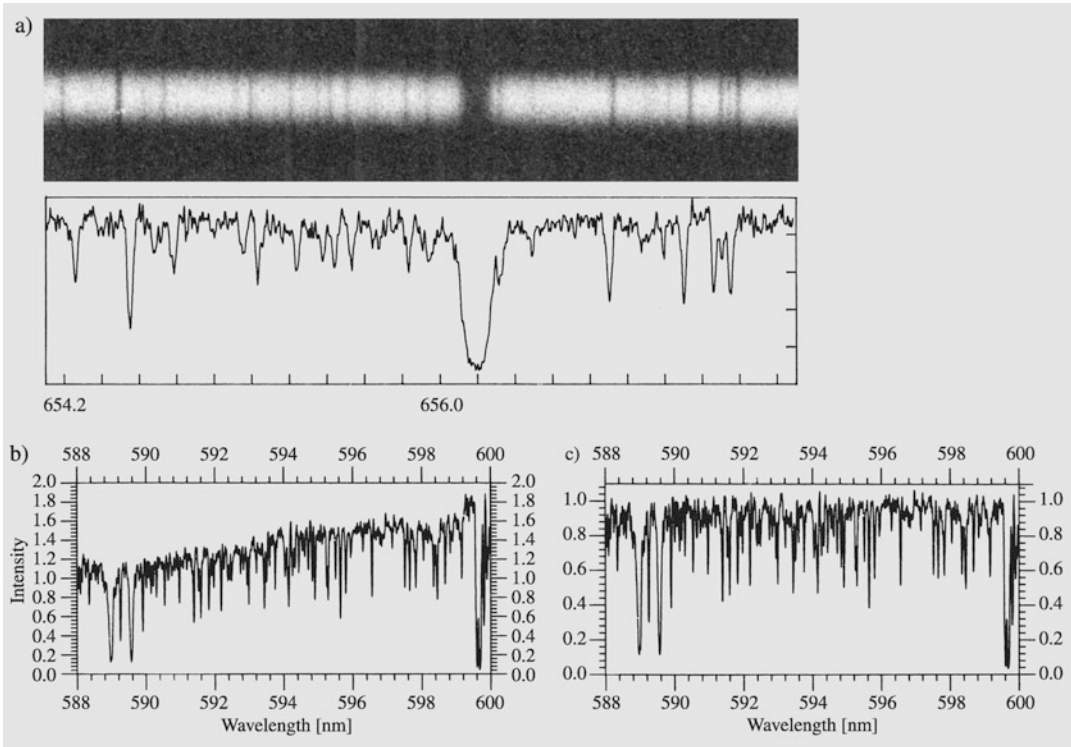


**Fig. 9.2** (a) A section of a photograph of a stellar spectrum and the corresponding rectified microdensitometer intensity tracing. The original spectrum was taken at the Crimean Observatory. (b) A more extensive part of the

spectrum. (c) The picture the intensity curve of the first picture has been rectified by normalising the value of the continuum intensity to one. (Pictures by J. Kyröläinen and H. Virtanen, Helsinki Observatory)

ceived, the measured blackening has to be calibrated by comparison with known exposures.

Nowadays CCD cameras are used also in spectrographs and the intensity curve is determined directly without the intervening step of a photographic plate. Some image processing is still needed since the height of the spectrum is several pixels and the spectrum may not be aligned with the pixel rows of the camera.

For measurements of line strengths the spectrum is usually rectified by dividing by the continuum intensity. Figure 9.2 shows a photograph of the spectrum of a star and the intensity curve obtained from a calibrated and rectified micro-

densitometer tracing. The second pair of pictures shows the intensity curve before and after the normalisation. The absorption lines appear as troughs of various sizes in the curve. In addition to the clear and deep lines, there are large numbers of weaker lines that can barely be discerned. The graininess of the photographic emulsion is a source of noise which appears as irregular fluctuations of the intensity curve. Some lines are so close together that they appear blended at this dispersion.

The detailed shape of a spectral line is called the *line profile* (Sect. 5.3). The true shape of the line reflects the properties of the stellar atmo-

sphere, but the observed profile is also spread out by the measuring instrument. However, the total absorption in the line, usually expressed in terms of the *equivalent width*, is less sensitive to observational effects (see Fig. 5.6).

The equivalent width of a spectral line depends on how many atoms in the atmosphere are in a state in which they can absorb the wavelength in question. The more atoms there are, the stronger and broader the spectral line is. For example, a typical equivalent width of a metal line (Fe) in the solar spectrum is about 10 pm. Line widths are often expressed in ångströms ( $1 \text{ \AA} = 10^{-10} \text{ m} = 0.1 \text{ nm}$ ).

Only in weak lines the equivalent width depends linearly on the number of absorbing atoms. The equivalent width as a function of the amount of absorbing atoms is known as the *curve of growth*. It is, however, beyond the scope of this book.

Line profiles are also broadened by the Doppler effect. In stellar atmospheres there are motions of small and large scale, like thermal motion of the atoms and convective flows.

The chemical composition of the atmosphere can be determined from the strengths of the spectral lines. With the introduction of large computers it has become feasible to construct quite detailed models of the structure of stellar atmospheres, and to compute the emergent spectrum for a given model. The computed synthetic spectrum can be compared with the observations and the theoretical model modified until a good fit is obtained. The theoretical models then give the number of absorbing atoms, and hence the element abundances, in the atmosphere. The construction of model atmospheres will be discussed in Sect. 9.6.

## 9.2 The Harvard Spectral Classification

The spectral classification scheme in present use was developed at Harvard Observatory in the United States in the early 20th century. The work was begun by *Henry Draper* who in 1872 took the first photograph of the spectrum of Vega. Later Draper's widow donated the observing

equipment and a sum of money to Harvard Observatory to continue the work of classification.

The main part of the classification was done by *Annie Jump Cannon* using objective prism spectra. The *Henry Draper Catalogue* (HD) was published in 1918–1924. It contains 225,000 stars extending down to 9 magnitudes. Altogether more than 390,000 stars were classified at Harvard.

The Harvard classification is based on lines that are mainly sensitive to the stellar temperature, rather than to gravity or luminosity. Important lines are the hydrogen Balmer lines, the lines of neutral helium, the iron lines, the H and K doublet of ionised calcium at 396.8 and 393.3 nm, the G band due to the CH molecule and some metals around 431 nm, the neutral calcium line at 422.7 nm and the lines of titanium oxide (TiO).

The main types in the Harvard classification are denoted by capital letters. They were initially ordered in alphabetical sequence, but subsequently it was noticed that they could be ordered according to temperature. With the temperature decreasing towards the right the sequence is

C  
O–B–A–F–G–K–M–L–T.  
S

Additional notations are Q for novae, P for planetary nebulae and W for Wolf–Rayet stars. The class C consists of the earlier types R and N. The spectral classes C and S represent parallel branches to types G–M, differing in their surface chemical composition. The most recent addition are the spectral classes L and T continuing the sequence beyond M, representing *brown dwarfs*. There is a well-known mnemonic for the spectral classes, but due to its chauvinistic tone we refuse to tell it.

The spectral classes are divided into subclasses denoted by the numbers 0, . . . , 9; sometimes decimals are used, e.g. B 0.5 (Figs. 9.3 and 9.4).

Classes at the beginning of the sequence are sometimes called *early classes* and those at the end of the sequence *late classes*. This is no way related to stellar evolution; it only reflects the position in the sequence O–B–A–F–G–K–M.

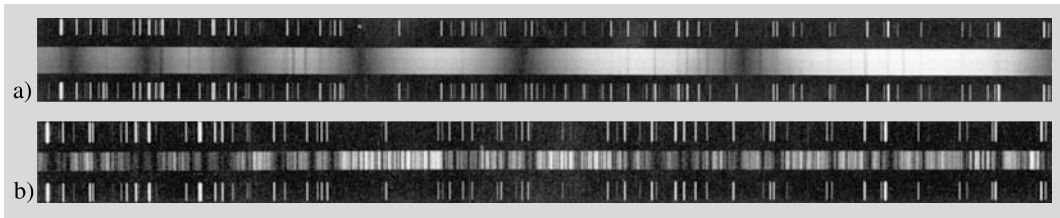


**Fig. 9.3** Spectra of early and late spectral type stars between 375 and 390 nm. (a) The upper star is Vega, of spectral type A0, and (b) the lower one is Aldebaran, of

spectral type K5. The hydrogen Balmer lines are strong in the spectrum of Vega; in that of Aldebaran, there are many metal lines. (Lick Observatory)

Spectra of brown dwarfs are shown in Fig. 9.4 and compared with those of M dwarfs.

The main characteristics of the different classes are:

- O Blue stars, surface temperature 20,000–35,000 K. Spectrum with lines from multiply ionised atoms, e.g. He II, C III, N III, O III, Si V. He I visible, H I lines weak.
- B Blue-white stars, surface temperature about 15,000 K. He II lines have disappeared, He I (403 nm) lines are strongest at B2, then get weaker and have disappeared at type B9. The K line of Ca II becomes visible at type B3. H I lines getting stronger. O II, Si II and Mg II lines visible.
- A White stars, surface temperature about 9000 K. The H I lines are very strong at A0 and dominate the whole spectrum, then get weaker. H and K lines of Ca II getting stronger. He I no longer visible. Neutral metal lines begin to appear.
- F Yellow-white stars, surface temperature about 7000 K. H I lines getting weaker, H and K of Ca II getting stronger. Many other metal lines, e.g. Fe I, Fe II, Cr II, Ti II, clear and getting stronger.
- G Yellow stars like the Sun, surface temperature about 5500 K. The H I lines still getting weaker, H and K lines very strong, strongest at G0. Metal lines getting stronger. G band clearly visible. CN lines seen in giant stars.
- K Orange-yellow stars, surface temperature about 4000 K. Spectrum dominated by metal lines. H I lines insignificant. Ca I 422.7 nm clearly visible. Strong H and K lines and G band. TiO bands become visible at K5.
- M Red stars, surface temperature about 3000 K. TiO bands getting stronger. Ca I 422.7 nm very strong. Many neutral metal lines.
- L Brown (actually dark red) stars, surface temperature about 2000 K. The TiO and VO bands disappear for early L class. Very strong and broad lines of Na I and K I.
- T Brown dwarfs, surface temperature about 1000 K. Very strong molecular absorption bands of CH<sub>4</sub> and H<sub>2</sub>O.
- C Carbon stars, previously R and N. Very red stars, surface temperature about 3000 K. Strong molecular bands, e.g. C<sub>2</sub>, CN and CH. No TiO bands. Line spectrum like in the types K and M.
- S Red low-temperature stars (about 3000 K). Very clear ZrO bands. Also other molecular bands, e.g. YO, LaO and TiO.

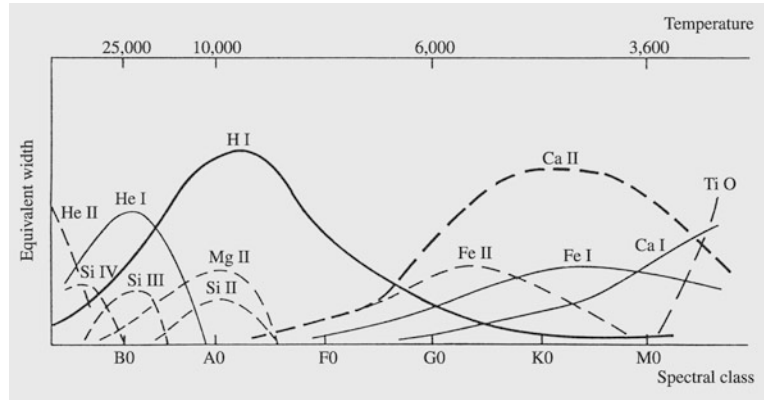
The main characteristics of the classification scheme can be seen in Fig. 9.5 showing the variations of some typical absorption lines in the different spectral classes. Different spectral features are mainly due to different effective temperatures. Different pressures and chemical compositions of stellar atmospheres are not very important factors in the spectral classification, except in some peculiar stars.

The early, i.e. hot, spectral classes are characterised by the lines of ionised atoms, whereas the cool, or late, spectral types have lines of neutral atoms. In hot stars molecules dissociate into atoms; thus the absorption bands of molecules appear only in the spectra of cool stars of late spectral types.

To see how the strengths of the spectral lines are determined by the temperature, we consider,



**Fig. 9.5** Equivalent widths of some important spectral lines in the various spectral classes. [Struve, O. (1959): *Elementary Astronomy* (Oxford University Press, New York) p. 259]



lium lines increases. When the temperature becomes even higher, helium begins to be ionised, and the strength of the neutral helium lines begins to decrease. In a similar way one can understand the variation with temperature of other important lines, such as the calcium H and K lines. These lines are due to singly ionised calcium, and the temperature must be just right to remove one electron but no more.

The hydrogen Balmer lines  $H_\beta$ ,  $H_\gamma$  and  $H_\delta$  are strongest in the spectral class A2. These lines correspond to transitions to the level the principal quantum number of which is  $n = 2$ . If the temperature is too high the hydrogen is ionised and such transitions are not possible.

### 9.3 The Yerkes Spectral Classification

The Harvard classification only takes into account the effect of the temperature on the spectrum. For a more precise classification, one also has to take into account the luminosity of the star, since two stars with the same effective temperature may have widely different luminosities.

A two-dimensional system of spectral classification was introduced by *William W. Morgan*, *Philip C. Keenan* and *Edith Kellman* of Yerkes Observatory. This system is known as the MKK or *Yerkes classification*. (The MK classification is a modified, later version.) The MKK classification is based on the visual scrutiny of slit spectra with a dispersion of 11.5 nm/mm. It is carefully defined on the basis of standard stars and the

specification of luminosity criteria. Six different *luminosity classes* are distinguished:

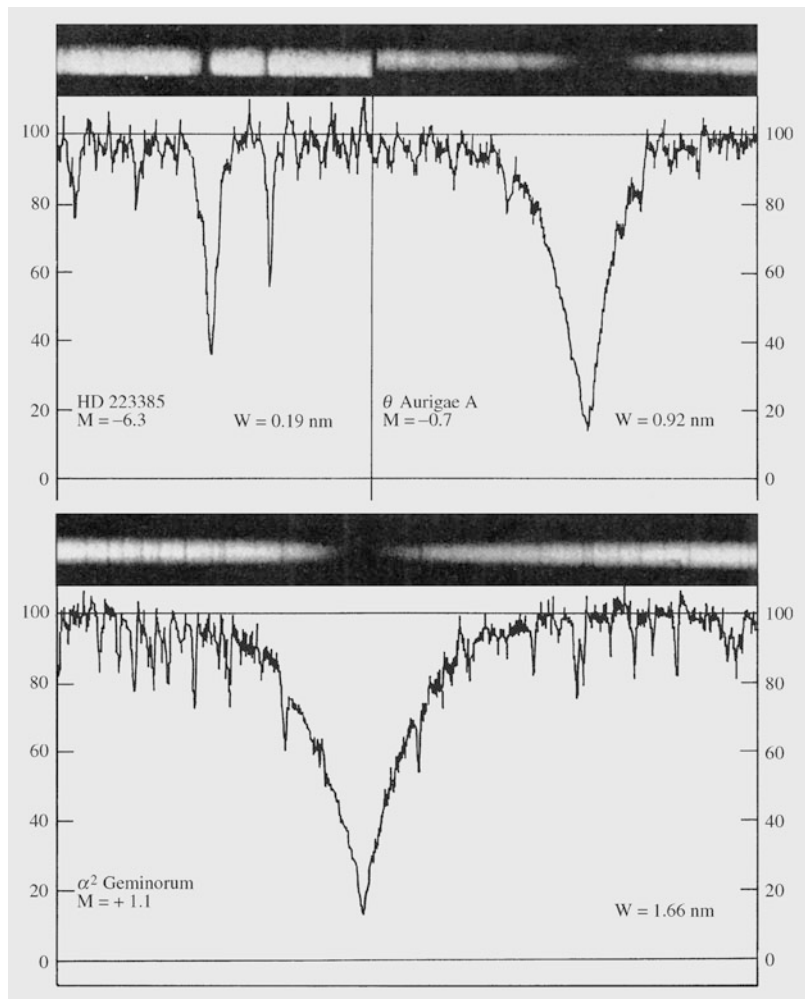
- Ia most luminous supergiants,
- Ib less luminous supergiants,
- II luminous giants,
- III normal giants,
- IV subgiants,
- V main sequence stars (dwarfs).

The luminosity class is denoted by a Roman numeral after the spectral class. For example, the class of the Sun is G2 V.

The luminosity class is determined from spectral lines that depend strongly on the stellar surface gravity, which is closely related to the luminosity. The masses of giants and dwarfs are roughly similar, but the radii of giants are much larger than those of dwarfs. Therefore the gravitational acceleration  $g = GM/R^2$  at the surface of a giant is much smaller than for a dwarf. In consequence, the gas density and pressure in the atmosphere of a giant is much smaller. This gives rise to *luminosity effects* in the stellar spectrum, which can be used to distinguish between stars of different luminosities.

1. For spectral types B–F, the lines of neutral hydrogen are deeper and narrower for stars of higher luminosities. The reason for this is that the metal ions give rise to a fluctuating electric field near the hydrogen atoms. This field leads to shifts in the hydrogen energy levels (the Stark effect), appearing as a broadening of the lines. The effect becomes stronger as the density increases. Thus the hydrogen lines

**Fig. 9.6** Luminosity effects in the hydrogen  $H_\gamma$  line in A stars. The vertical axis gives the normalised intensity. HD 223385 (upper left) is an A2 supergiant, where the line is very weak,  $\theta$  Aurigae A is a giant star and  $\alpha^2$  Geminorum is a main sequence star, where the line is very broad. [Aller, L.H. (1953): *Astrophysics. The Atmospheres of the Sun and Stars* (The Ronald Press Company, New York) p. 318]



are narrow in absolutely bright stars, and become broader in main sequence stars and even more so in white dwarfs (Fig. 9.6).

2. The lines from ionised elements are relatively stronger in high-luminosity stars. This is because the higher density makes it easier for electrons and ions to recombine to neutral atoms. On the other hand, the rate of ionisation is essentially determined by the radiation field, and is not appreciably affected by the gas density. Thus a given radiation field can maintain a higher degree of ionisation in stars with more extended atmospheres. For example, in the spectral classes F–G, the relative strengths of the ionised strontium (Sr II) and neutral iron (Fe I) lines can be used as a luminosity indicator. Both lines depend on the temperature in roughly the same way, but the Sr II lines become relatively much stronger as the luminosity increases.
3. Giant stars are redder than dwarfs of the same spectral type. The spectral type is determined from the strengths of spectral lines, including ion lines. Since these are stronger in giants, a giant will be cooler, and thus also redder, than a dwarf of the same spectral type.
4. There is a strong cyanogen (CN) absorption band in the spectra of giant stars, which is almost totally absent in dwarfs. This is partly a temperature effect, since the cooler atmospheres of giants are more suitable for the formation of cyanogen.

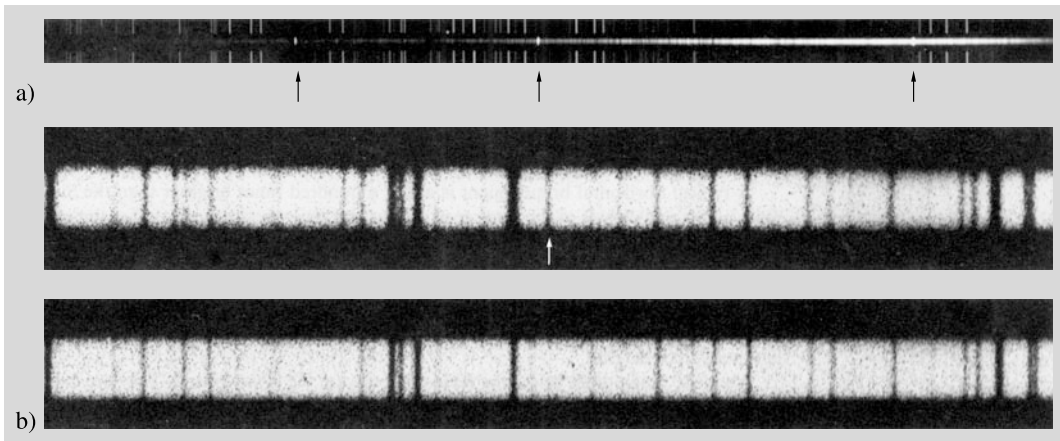


**Fig. 9.7** Peculiar spectra. (a) R Geminorum (*above*) is an emission line star, with bright emission lines, indicated by arrows, in its spectrum; (b) the spectrum of a normal star

is compared with one in which the zirconium lines are unusually strong. (Mt. Wilson Observatory and Helsinki Observatory)

## 9.4 Peculiar Spectra

The spectra of some stars differ from what one would expect on the basis of their temperature and luminosity (see, e.g., Fig. 9.7). Such stars are called *peculiar*. The most common peculiar spectral types will now be considered.

The *Wolf-Rayet stars* are very hot stars; the first examples were discovered by *Charles Wolf* and *Georges Rayet* in 1867. The spectra of Wolf-Rayet stars have broad emission lines of hydrogen and ionised helium, carbon, nitrogen and oxygen. There are hardly any absorption lines. The Wolf-Rayet stars are thought to be very massive stars that have lost their outer layers in a strong stellar wind. This has exposed the stellar interior, which gives rise to a different spectrum than the normal outer layers. Many Wolf-Rayet stars are members of binary systems.

In some O and B stars the hydrogen absorption lines have weak emission components either at the line centre or in its wings. These stars are called *Be* and *shell stars* (the letter e after the spectral type indicates that there are emission lines in the spectrum). The emission lines are formed in a rotationally flattened gas shell around the star. The shell and Be stars show irregular variations, apparently related to structural changes in the shell. About 15 % of all O and B stars have emission lines in their spectra.

The strongest emission lines are those of the *P Cygni* stars, which have one or more sharp absorption lines on the short wavelength side of the emission line. It is thought that the lines are formed in a thick expanding envelope. The P Cygni stars are often variable. For example, P Cygni itself has varied between three and six magnitudes during the past centuries. At present its magnitude is about 5.

The peculiar A stars or *Ap stars* ( $p = \text{peculiar}$ ) are usually strongly magnetic stars, where the lines are split into several components by the Zeeman effect. The lines of certain elements, such as magnesium, silicon, europium, chromium and strontium, are exceptionally strong in the Ap stars. Lines of rarer elements such as mercury, gallium or krypton may also be present. Otherwise, the Ap stars are like normal main sequence stars.

The *Am stars* ( $m = \text{metallic}$ ) also have anomalous element abundances, but not to the same extent as the Ap stars. The lines of e.g. the rare earths and the heaviest elements are strong in their spectra; those of calcium and scandium are weak.

We have already mentioned the S and C stars, which are special classes of K and M giants with anomalous element abundances. In the S stars, the normal lines of titanium, scandium and vanadium oxide are replaced with oxides of heavier



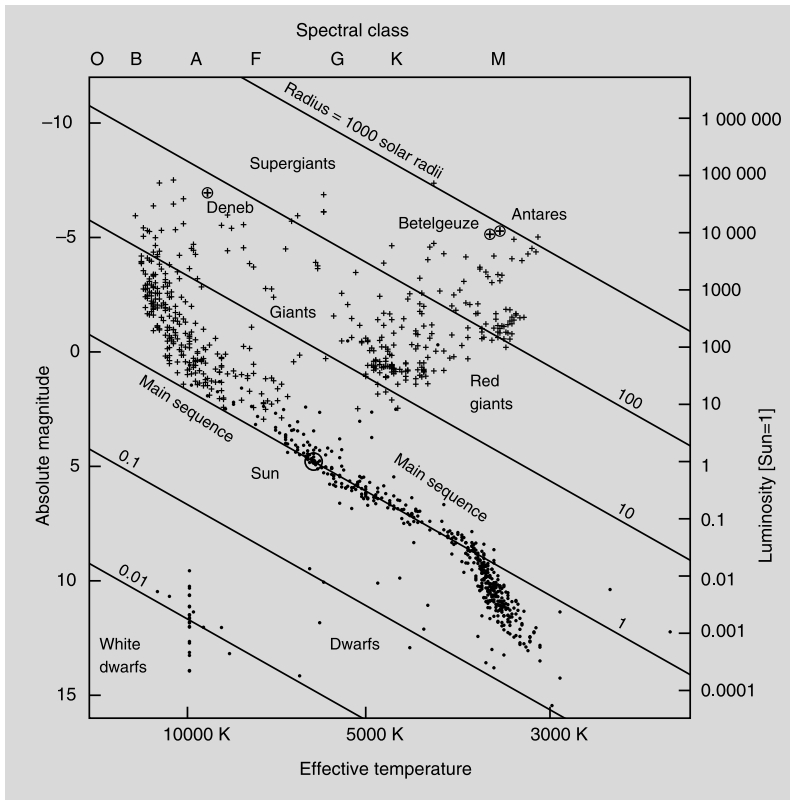


**Fig. 9.8** The Hertzsprung–Russell diagram. The horizontal coordinate can be either the colour index  $B - V$ , obtained directly from observations, or the spectral class. In theoretical studies the effective temperature  $T_e$  is commonly used. These correspond to each other but the dependence varies somewhat with luminosity. The vertical axis gives the absolute magnitude. In a  $(\lg(L/L_\odot), \lg T_e)$  plot the curves of constant radius are straight lines. The dens-

*est areas* are the main sequence and the horizontal, red giant and asymptotic branches consisting of giant stars. The supergiants are scattered above the giants. To the lower left are some white dwarfs about 10 magnitudes below the main sequence. The apparently brightest stars ( $m < 4$ ) are marked with crosses and the nearest stars ( $r < 50$  ly) with dots. The data are from the Hipparcos catalogue

elements, zirconium, yttrium and barium. A large fraction of the S stars are irregular variables. The name of the C stars refers to carbon. The metal oxide lines are almost completely absent in their spectra; instead, various carbon compounds (CN, C<sub>2</sub>, CH) are strong. The abundance of carbon relative to oxygen is 4–5 times greater in the C stars than in normal stars. The C stars are divided into two groups, hotter R stars and cooler N stars.

Another type of giant stars with abundance anomalies are the *barium stars*. The lines of barium, strontium, rare earths and some carbon compounds are strong in their spectra. Apparently nuclear reaction products have been mixed up to the surface in these stars.

## 9.5 The Hertzsprung–Russell Diagram

Around 1910, *Ejnar Hertzsprung* and *Henry Norris Russell* studied the relation between the absolute magnitudes and the spectral types of stars. The diagram showing these two variables is now known as the *Hertzsprung–Russell diagram* or simply the *HR diagram* (Fig. 9.8). It has turned out to be an important aid in studies of stellar evolution.

In view of the fact that stellar radii, luminosities and surface temperatures vary widely, one might have expected the stars to be uniformly distributed in the HR diagram. However, it is found

that most stars are located along a roughly diagonal curve called the *main sequence*. The Sun is situated about the middle of the main sequence.

The HR diagram also shows that the yellow and red stars (spectral types G–K–M) are clustered into two clearly separate groups: the *main sequence* of *dwarf stars* and the *giants*. The giant stars fall into several distinct groups. The *horizontal branch* is an almost horizontal sequence, about absolute visual magnitude zero. The *red giant branch* rises almost vertically from the main sequence at spectral types K and M in the HR diagram. Finally, the *asymptotic branch* rises from the horizontal branch and approaches the bright end of the red giant branch. These various branches represent different phases of stellar evolution (cf. Sects. 12.3 and 12.4): dense areas correspond to evolutionary stages in which stars stay a long time.

A typical horizontal branch giant is about a hundred times brighter than the Sun. Since giants and dwarfs of the same spectral class have nearly the same surface temperature, the difference in luminosity must be due to a difference in radius according to (5.21). For example Arcturus, which is one of the brightest stars in the sky, has a radius about thirty times that of the Sun.

The brightest red giants are the *supergiants* with magnitudes up to  $M_V = -7$ . One example is Betelgeuze, in Orion, with a radius of 400 solar radii and 20,000 times more luminous than the Sun.

About 10 magnitudes below the main sequence are the *white dwarfs*. They are quite numerous in space, but faint and difficult to find. The best-known example is Sirius B, the companion of Sirius.

There are some stars in the HR diagram which are located below the giant branch, but still clearly above the main sequence. These are known as *subgiants*. Similarly, there are stars below the main sequence, but brighter than the white dwarfs, known as *subdwarfs*.

When interpreting the HR diagram, one has to take into account *selection effects*: absolutely bright stars are more likely to be included in the sample, since they can be discovered at greater distances. If only stars within a certain distance

from the Sun are included, the distribution of stars in the HR diagram looks quite different. This can be seen in Fig. 9.8: there are no giant or bright main sequence stars among these.

The HR diagrams of star clusters are particularly important for the theory of stellar evolution. They will be discussed in Chap. 17.

---

## 9.6 Model Atmospheres

The stellar atmosphere consists of those layers of the star where the radiation that is transmitted directly to the observer originates. Thus in order to interpret stellar spectra, one needs to be able to compute the structure of the atmosphere and the emerging radiation.

In actual stars there are many factors, such as rotation and magnetic fields, that complicate the problem of computing the structure of the atmosphere. We shall only consider the classical problem of finding the structure, i.e. the distribution of pressure and temperature with depth, in a static, unmagnetised atmosphere. In that case a model atmosphere is completely specified by giving the chemical composition, the gravitational acceleration at the surface,  $g$ , and the energy flux from the stellar interior, or equivalently, the effective temperature  $T_e$ .

The basic principles involved in computing a model stellar atmosphere are the same as for stellar interiors and will be discussed in Chap. 11. Essentially, there are two differential equations to be solved: the equation of hydrostatic equilibrium, which fixes the distribution of pressure, and an equation of energy transport, which will have a different form depending on whether the atmosphere is radiative or convective, and which determines the temperature distribution.

The values of the various physical quantities in an atmosphere are usually given as functions of some suitably defined continuum optical depth  $\tau$ . Thus pressure, temperature, density, ionisation and the population numbers of various energy levels can all be obtained as functions of  $\tau$ . When these are known, the intensity of radiation emerging from the atmosphere can be computed. In Box 9.1, it is shown that approximately the emergent spectrum originates at unit optical depth,

measured along each light ray. On this basis, one can predict whether a given spectral line will be present in the spectrum.

Consider a spectral line formed when an atom (or ion) in a given energy state absorbs a photon. From the model atmosphere, the occupation number of the absorbing level is known as a function of the (continuum) optical depth  $\tau$ . If now there is a layer above the depth  $\tau = 1$  where the absorbing level has a high occupancy, the optical depth in the line will become unity before  $\tau = 1$ , i.e. the radiation in the line will originate higher in the atmosphere. Because the temperature increases inwards, the intensity in the line will correspond to a lower temperature, and the line will appear dark. On the other hand, if the absorbing level is unoccupied, the optical depth at the line frequency will be the same as the continuum optical depth. The radiation at the line frequency will then come from the same depth as the adjacent continuum, and no absorption line will be formed.

The expression for the intensity derived in Box 9.1 also explains the phenomenon of *limb darkening* seen in the Sun (Sect. 12.2). The radiation that reaches us from near the edge of the solar disk emerges at a very oblique angle ( $\theta$  near  $90^\circ$ ), i.e.  $\cos \theta$  is small. Thus this radiation originates at small values of  $\tau$ , and hence at low temperatures. In consequence, the intensity coming from near the edge will be lower, and the solar disk will appear darker towards the limb. The amount of limb darkening also gives an empirical way of determining the temperature distribution in the solar atmosphere.

Our presentation of stellar atmospheres has been highly simplified. In practice, the spectrum is computed numerically for a range of parameter values. The values of  $T_e$  and element abundances for various stars can then be found by comparing the observed line strengths and other spectral features with the theoretical ones. We shall not go into details on the procedures used.

## 9.7 What Do the Observations Tell Us?

To conclude this chapter, we shall give a summary of the properties of stars revealed by the ob-

servations. At the end of the book, there are tables of the brightest and of the nearest stars.

Of the brightest stars, four have a negative magnitude. Some of the apparently bright stars are absolutely bright supergiants, others are simply nearby.

In the list of the nearest stars, the dominance of faint dwarf stars, already apparent in the HR diagram, is worth noting. Most of these belong to the spectral types K and M. Some nearby stars also have very faint companions with masses about that of Jupiter, i.e. planets. They have not been included in the table.

Stellar spectroscopy offers an important way of determining fundamental stellar parameters, in particular mass and radius. However, the spectral information needs to be calibrated by means of direct measurements of these quantities. These will be considered next.

The *masses* of stars can be determined in the case of double stars orbiting each other. (The details of the method will be discussed in Chap. 9.) These observations have shown that the larger the mass of a main sequence star becomes, the higher on the main sequence it is located. One thus obtains an empirical *mass–luminosity relation*, which can be used to estimate stellar masses on the basis of the spectral type.

The observed relation between mass and luminosity is shown in Fig. 9.9. The luminosity is roughly proportional to the power 3.8 of the mass:

$$L \propto M^{3.8}. \quad (9.1)$$

The relation is only approximate. According to it, a ten solar mass star is about 6300 times brighter than the Sun, corresponding to 9.5 magnitudes.

The smallest observed stellar masses are about 1/20 of the solar mass, corresponding to stars in the lower right-hand part of the HR diagram. The masses of white dwarfs are less than one solar mass. The masses of the most massive main sequence and supergiant stars are between 10 and possibly even  $150 M_\odot$ .

Direct interferometric measurements of stellar angular diameters have been made for only a few dozen stars. When the distances are known, these immediately yield the value of the radius. In

eclipsing binaries, the radius can also be directly measured (see Sect. 10.4). Altogether, close to a hundred stellar radii are known from direct measurements. In other cases, the radius must be estimated from the absolute luminosity and effective temperature.

In discussing stellar radii, it is convenient to use a version of the HR diagram with  $\lg T_e$  on the horizontal and  $M_{\text{bol}}$  or  $\lg(L/L_\odot)$  on the vertical axis. If the value of the radius  $R$  is fixed, then (5.21) yields a linear relation between the bolometric magnitude and  $\lg T_e$ . Thus lines of constant radius in the HR diagram are straight. Lines corresponding to various values of the radius are shown in Fig. 9.8. The smallest stars are the white dwarfs with radii of about one per cent of the so-

lar radius, whereas the largest supergiants have radii several thousand times larger than the Sun. Not included in the figure are the compact stars (neutron stars and black holes) with typical radii of a few tens of kilometres.

Since the stellar radii vary so widely, so do the densities of stars. The density of giant stars may be only  $10^{-4} \text{ kg/m}^3$ , whereas the density of white dwarfs is about  $10^9 \text{ kg/m}^3$ .

The range of values for stellar effective temperatures and luminosities can be immediately seen in the HR diagram. The range of effective temperature is 2000–40,000 K, and that of luminosity  $10^{-4}$ – $10^6 L_\odot$ .

The *rotation* of stars appears as a broadening of the spectral lines. One edge of the stellar disk is approaching us, the other edge is receding, and the radiation from the edges is Doppler shifted accordingly. The rotational velocity observed in this way is only the component along the line of sight. The true velocity is obtained by dividing with  $\sin i$ , where  $i$  is the angle between the line of sight and the rotational axis. A star seen from the direction of the pole will show no rotation.

Assuming the axes of rotation to be randomly oriented, the distribution of rotational velocities can be statistically estimated. The hottest stars appear to rotate faster than the cooler ones. The rotational velocity at the equator varies from 200–250 km/s for O and B stars to about 20 km/s for spectral type G. In shell stars, the rotational velocity may reach 500 km/s.

The *chemical composition* of the outer layers is deduced from the strengths of the spectral lines. About three-fourths of the stellar mass is hydrogen. Helium comprises about one-fourth, and the abundance of other elements is very small. The abundance of heavy elements in young stars (about 2 %) is much larger than in old ones, where it is less than 0.02 %.

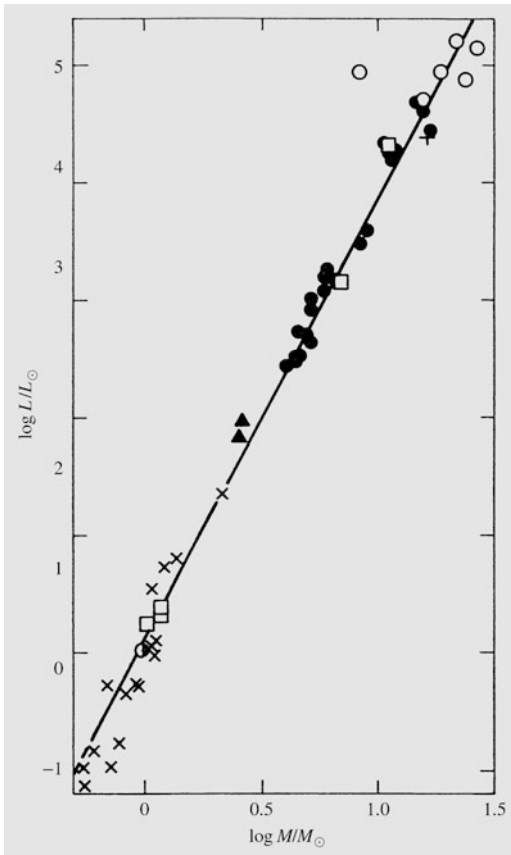


**Fig. 9.9** Mass–luminosity relation. The picture is based on binaries with known masses. Different symbols refer to different kinds of binaries. (From Böhm-Vitense: *Introduction to Stellar Astrophysics*, Cambridge University Press (1989–1992))

**Box 9.1** (The Intensity Emerging from a Stellar Atmosphere) The intensity of radiation emerging from an atmosphere is given by the expression (5.45), i.e.

$$I_\nu(0, \theta) = \int_0^\infty S_\nu(\tau_\nu) e^{-\tau_\nu \sec \theta} \sec \theta \, d\tau_\nu. \quad (9.2)$$

If a model atmosphere has been computed, the source function  $S_\nu$  is known.

An approximate formula for the intensity can be derived as follows. Let us expand the source function as a Taylor series about some arbitrary point  $\tau^*$ , thus

$$S_\nu = S_\nu(\tau^*) + (\tau_\nu - \tau^*)S'_\nu(\tau^*) + \dots$$

where the dash denotes a derivative. With this expression, the integral in (9.2) can be evaluated, yielding

$$I_\nu(0, \theta) = S_\nu(\tau^*) + (\cos \theta - \tau^*)S'_\nu(\tau^*) + \dots$$

If we now choose  $\tau^* = \cos \theta$ , the second term will vanish. In local thermodynamic

equilibrium the source function will be the Planck function  $B_\nu(T)$ . We thus obtain the *Eddington–Barbier approximation*

$$I_\nu(0, \theta) = B_\nu(T[\tau_\nu = \cos \theta]).$$

According to this expression, the radiation emerging in a given direction originated at unit optical depth along that direction.

### 9.8 Exercise

**Exercise 9.1** Arrange the below spectra in the order of decreasing temperature.

